

Decolorization of C.I. Reactive Red 124 Using the Electrocoagulation Method

I. A. Şengil^{*a}, M. Özacar^b, and Beyza Ömürlü^c

^aDepartment of Environmental Engineering, Engineering Faculty, Sakarya University, 54100 Sakarya–TURKEY

^bDepartment of Chemistry, Science & Arts Faculty, Sakarya University, 54100 Sakarya–TURKEY

^cInstitute of Sciences and Technology, Sakarya University

Original scientific paper

Received: March 31, 2004

Accepted: September 23, 2004

The removal of color from synthetic wastewater containing a reactive dye, C.I. reactive red 124, was experimentally investigated using direct current (D.C.) electrocoagulation (EC). In the EC of the reactive dye the effects of initial pH, electrolysis time, initial concentration of dye, conductivity and current density, were examined. The dye in the aqueous phase were effectively removed when iron was used as sacrificial anode. The optimum operating range for each operating variable was experimentally determined. The batch experimental results were assessed in terms of color. They revealed that the color of the reactive dye in aqueous phase was effectively removed (100 %). The optimum current density, pH and electrolysis time for 100 mg L⁻¹ initial dye mass concentration were 1.351 mA cm⁻², 8 and 5 min, respectively.

Key words:

D.C. electrocoagulation (EC), iron electrode, reactive dye, C.I. reactive red 124

Introduction

The large quantity of aqueous waste generated by textile industries has become a significant environmental problem. The water employed in the dyeing and finishing processes eventually ends up as wastewater that needs to be treated before final discharge. Colored wastewater is not only an inherent feature of textile discharges; it is produced also in other industrial operations such as coffee absorption, yeast preparation, and edible oil refinery. Strong color and turbidity of the wastewater effluents are particularly troublesome because of its negative visual impact. Because dyes absorb sunlight, plants in sewage streams may perish; thus the ecosystem of streams could be seriously affected.¹

The characteristics of wastewater from textile dyeing are high or low pH, high temperature and a high concentration of coloring material. The methods of treatment of dyeing wastewater are biological treatment, chemical coagulation, activated carbon adsorption, ultrafiltration, ozonation and EC.^{2–10}

In recent years, EC has been successfully tested to treat various industrial wastewater^{11–19}.

Electrochemical methods have been used as chemical coagulation processes to remove color and cloudiness from colored industrial wastewater. In

this regard, it has been observed that the electrochemical process generated numerous flocs, which permitted to attain high efficiency in clearing wastewater. The electrochemical technologies have attracted a great deal of attention because of their versatility and environmental compatibility, which makes the treatments of liquids, gases and solids possible. In fact, the main reagent is the electron, which is a “clean reagent”.²⁰ A host of very promising techniques based on electrochemical technology, that do not require chemical additions, are being developed and existing ones improved. These include EC, electroflotation and electrodecantation. EC is a process consisting of creating a floc of metallic hydroxides within the effluent to be cleaned, by electrodisolution of soluble anodes. Iron and aluminium are generally used as sacrificial anodes.^{21–24}

In recent years, EC has been successfully tested to treat decolorization of dye-containing solutions. The dye in dye-containing wastewater is coagulated by iron (II) and aluminium hydrates or hydroxides produced from the sacrificial anode.^{2,25–32}

In this paper the EC of a reactive dye, C.I. reactive red 124, in aqueous solutions using an iron sacrificial anode, is described. Our aim was to investigate the decolorization by EC of the solutions containing a reactive dye and to determine the influence on decolorization process of the operating variables such as current density, pH, conductivity, initial dye concentration, and electrolysis time.

*Corresponding author: Prof. Dr. I. Ayhan Şengil, Sakarya University, Engineering Faculty, Department of Environmental Engineering, 54100 Sakarya – TURKEY; Fax: 00. 90. 264. 2762059; e-mail address : ayhansengil@hotmail.com

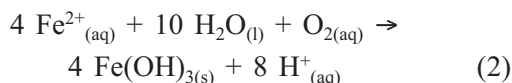
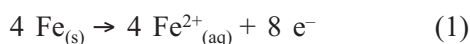
A brief description of electrocoagulation mechanism

First of all, decolorization of solutions containing C.I. reactive red 124, by using iron and aluminum electrode materials was investigated. The results show that iron is superior to aluminum as sacrificial electrode material. In this respect, iron electrodes were used in all experiments.

The Fe (II) ions are the common ions generated by the dissolution of iron. In contrast, OH⁻ ions are produced at the cathode. By mixing the solution, hydroxide species are produced which cause the removal of matrices (dyes and cations) by adsorption and coprecipitation. In the study of iron anodes, two mechanisms for the production of the metal hydroxides have been proposed:²²

Mechanism 1:

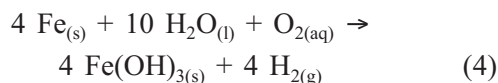
Anode:



Cathode:

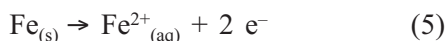


Overall:

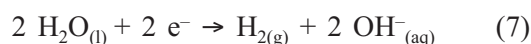


Mechanism 2:

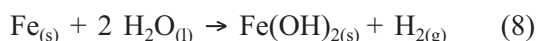
Anode:



Cathode:



Overall :



The Fe(OH)_{n(s)} formed remains in the aqueous stream as a gelatinous suspension, which can remove the dye from wastewater either by complexation or by electrostatic attraction followed by coagulation.

Ferric ions electrogenerated may form monomeric ions, ferric hydroxo complexes with hydroxide ions and polymeric species, namely, Fe(H₂O)₆³⁺, Fe(H₂O)₅OH²⁺, Fe(H₂O)₄(OH)₂¹⁺, Fe₂(H₂O)₈(OH)₂⁴⁺, Fe₂(H₂O)₆(OH)₄²⁺ and Fe(OH)₄⁻ depending on the

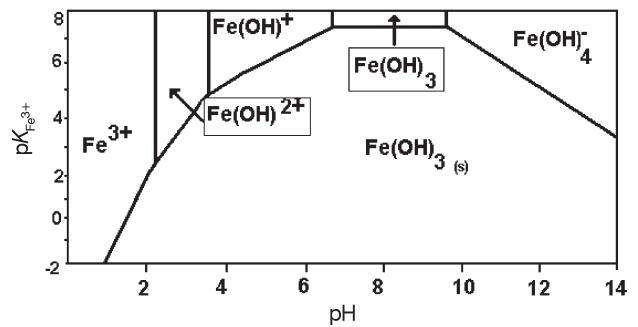


Fig. 1 – Predominance-zone diagrams for Fe(III) chemical species in aqueous solution. Note that, in this case, the solid line represents the solubility equilibrium of Fe(OH)₃ and the dotted line represents the predominance limits among soluble chemical species.^{19,20}

pH range.³¹ The complexes (i.e. hydrolysis products) have a pronounced tendency to polymerize at pH 3.5–7.0. A solubility diagram for Fe(III) in water is presented in Fig. 1.^{19,20}

Materials and methods

Reactive dye

The dye used in the experiments was C.I. reactive red 124. This dye was of commercial grade and was used without further purification. All concentrations were measured at the wavelength corresponding to maximum absorbance, λ_{max}, which for C.I. reactive red 124 is 544 nm, and using spectrophotometer (Shimadzu UV-150-02). The characteristic schematic structure of a reactive dye was shown in Figure 2. The reactive group (halogen atom) of the dye forms a covalent bond with the functional groups of textile fibres. These functional groups are hydroxyl, amino, carboxyl and thioalcohol group. Reactive dyes form generally strong covalent bonds in base solutions.³³

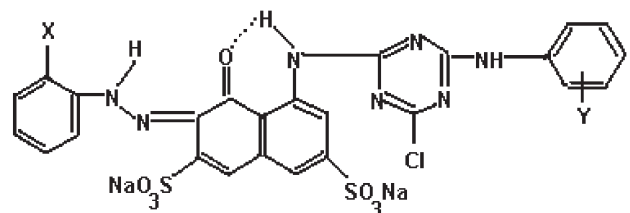


Fig. 2 – The characteristic schematic structure of a reactive dye

Electrochemical reactor

The batch experimental setup is schematically shown in Fig. 3. The EC unit consists of an electrochemical reactor, a D.C. power supply and iron electrodes. The iron cathode and iron anode consist of pieces of cast iron separated by a space of 2.5 cm

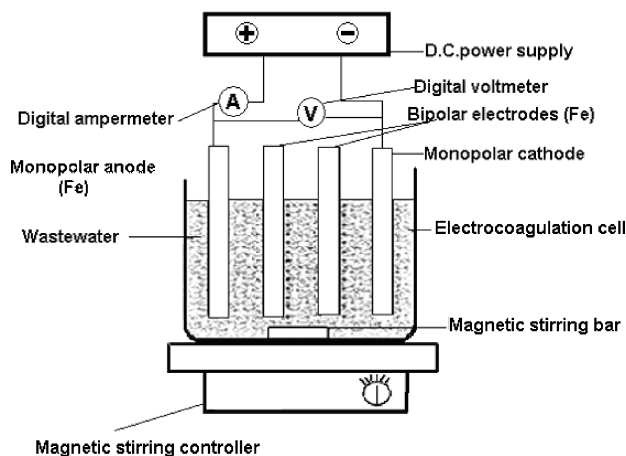


Fig. 3 – Bench-scale EC reactor with bipolar electrodes in parallel connection

and dipped in the wastewater. The EC of dye containing aqueous solutions was carried out in the reactor (650 ml) using magnetic stirrers to agitate the solutions. There were 4 electrodes connected in a bipolar mode in the electrochemical reactor, each one with dimensions of $10 \times 5 \times 0.2$ cm. The total area of the electrode plates was 0.0106 m^2 . The stirrer was used in the electrochemical cell to maintain an unchanged composition and avoid the association of the flocs in the solution. The D.C. source was used to power supply the system with 0–15 V and 0–3 A.

Synthetic wastewater samples and experimental procedure

The synthetic wastewater containing the reactive dye was prepared using distilled water. Concentrations of the dye were 100, 200, 300, 400 and 500 mg L^{-1} . The pH and conductivity were adjusted to a desirable value using HCl, NaOH and NaCl. The salt mass concentrations for conductivity were 0.77, 1.54, 2.30, 3.07, 4.61 mg L^{-1} . pH and current density values were 4, 6, 7, 8, 10 and $0.675, 1.351, 2.030, 2.700 \text{ mA cm}^{-2}$, respectively.

At the beginning of a run the desired concentration of dye in the aqueous solution was fed into the reactor and the pH and conductivity were adjusted to a desired value. The iron electrodes were placed into the reactor. The reaction was timed, starting when the D.C. power supply was switched on.

Iron salts produce electrode passivation and it causes a 50 % increase in treatment time and power requirements. Eliminating the salt formation at the anode could reduce this effect.^{34,35} For this reason, the electrodes were rinsed in the diluted HCl solution after the each experiment.

Samples were periodically taken from the reactor. The particulates of colloidal ferric oxyhydroxides gave yellow–brown colour into the solution

after EC. The precipitate in the sample was centrifugated at 1000 rpm for 15 min and the supernatant liquid was decanted. The dye concentrations were measured at the wavelength corresponding to maximum absorbance, λ_{max} , using a spectrophotometer (Shimadzu UV–150–02).

Sludge characterization

The quantity of sludge generated by the electrochemical technique is lower than the chemical method. Furthermore, morphologies of sludges are different, while the sludge generated by the chemical technique appear to be dense and large, the sludge generated electrochemically form clusters.¹⁹

The sludge produced by the electrochemical processes was analyzed by FTIR. Following, EC produced sludge was filtered through $0.45 \mu\text{m}$ Millipore membrane filters. The remaining part was dried at 378 K. Sample pellets were prepared by mixing 1mg of dried sludge with 200 mg of KBr (spectrometry grade) at 980.66 kPa ($10.000 \text{ kg cm}^{-2}$) pressure for 30 min under vacuum. FTIR spectra were recorded from 2000 to 400 cm^{-1} (100 scans) using a Mattson Infinity Series FTIR spectrophotometer.

Results and discussion

Effect of initial pH

Effect of initial pH on the removal efficiency of reactive dye

It has been established that pH is an important parameter influencing the performance of the EC process.¹⁰ To examine its effect, the sample was adjusted to a desired pH for each experiment by using sodium hydroxide or hydrochloric acid. Figure 4 shows the removal efficiency of reactive dye as a function of the initial pH. pH of the medium increased during the process. The maximum removals of reactive dye were observed at pH around 8 for 3 min electrolysis duration and 2.030 mA cm^{-2} current density. Best removal results for 5 min electrolysis duration were observed at a pH of 6 to 10 and 2.030 mA cm^{-2} . However, at 2.700 mA cm^{-2} of current density, it is clear from Fig.4a that a good result is reached from pH 7 to 10 for 3 min electrolysis duration and from pH 3.5 to 10 for 5 min electrolysis duration (as seen on Fig. 4b). The removal of the reactive dye in this pH region was 100 %.

The mechanism of decolorization

The mechanism of the EC process in aqueous systems is quite complex. The color removal process may involve adsorption of the dye molecule by

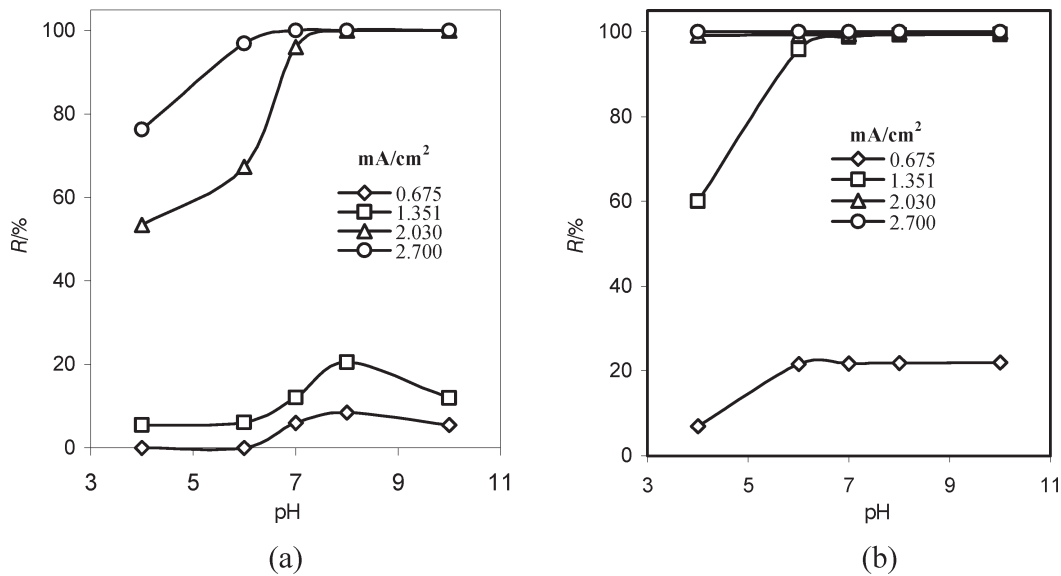


Fig. 4 – Effect of initial pH on the removal efficiency of reactive dye, R/%. (a) Duration of electrolysis $t = 3$ min; (b) Duration of electrolysis $t = 5$ min ($\gamma_0 = 100$ mg L⁻¹; $T = 298$ K; $d = 2.5$ cm; $\gamma_{NaCl} = 3$ g L⁻¹; rotation speed: $n_r = 100$ rpm)

both electrostatic attraction and physical entrapment. Also, the reactive group of the dye actually may form a covalent bond with the hydroxyl groups of the ferric hydroxo complexes. FTIR was used to monitor the EC mechanism. IR spectra of the C.I. reactive red 124 and of the ferric oxyhydroxides formed in EC of distilled water and sludge, formed after EC of dye solution are shown in Fig. 5. The characteristic frequencies of the important groups in the dye and ferric oxyhydroxides are listed in Table 1.

A comparison between the spectra of the reactive dye bonded with the ferric oxyhydroxides surface, during the EC and the spectra of the reactive dye and ferric oxyhydroxides alone, showed some changes in the frequencies and intensity of bands. Thus, there must be some changes in the conformation after the transfer of dye from the solution onto the ferric oxyhydroxides surface. The spectral peaks of the sludge formed in electrocoagulation in Fig 5c show different frequencies in the region 1600 ~ 467 cm⁻¹ according to the spectral peaks of

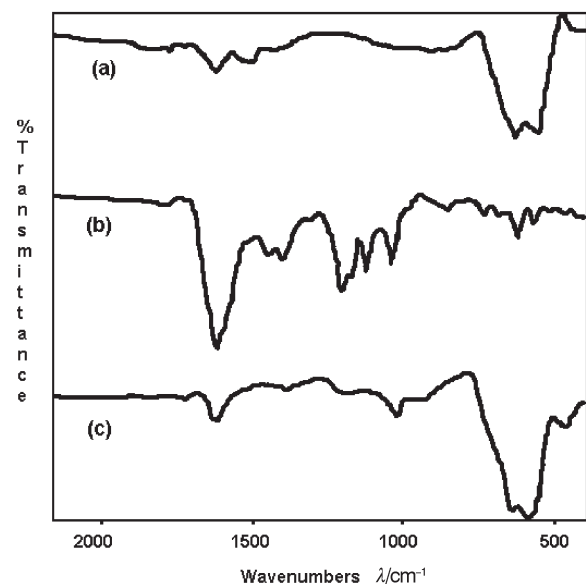
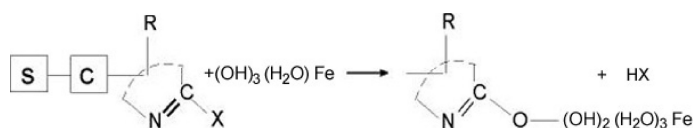


Fig. 5 – FTIR spectra of samples, recorded at room temperature. a) Ferric Oxyhydroxides b) Reactive dye (R.I. Reactive Red 124) c) The sludge formed in electrocoagulation

Table 1 – The characteristic IR frequencies of important groups and their actual frequencies^{41–44}

Group name	Group	R.I. Reactive Red 124 IR λ / cm ⁻¹	Ferric Oxyhydroxides IR λ / cm ⁻¹	The Sludge IR λ / cm ⁻¹
Sulphonates	Ar-SO ₃ ⁻	1208–1403	–	Disappeared
Chlorine	Ar-Cl	859–733	–	Disappeared
Vinly	-CH=CH ₂	623–569	–	Disappeared
Aromatic	C=C	1640	–	Diminished
Amine	N=C	1640	–	Diminished
Ferric Oxyhydroxide	α -FeOOH	–	630–700	630–700– Little extended

C.I. reactive red 124. The characteristic frequencies of the important groups as C=C, N=C, Ar-Cl, Ar-SO₃ and -CH=CH₂ were disappeared. As can be seen in Fig. 5, the bands at approximately 467 – 859 cm⁻¹ for the reactive dye showed significant changes. Namely, the Ar-Cl groups in the dye may interact with the ferric oxyhydroxides. The dye molecule is bound strongly to the ferric hydroxo complexes formed during electrocoagulation. It is assumed that the dye molecule can act as a ligand to bind a hydroxo complex.³³



As can be seen in Fig. 4, the removal efficiency of reactive dye at low pHs decreases. It is due to the fact that the reactive dye forms the covalent bond at high pHs. Also, at low pHs the solution protons are reduced at the cathode to H₂ and the same proportion of hydroxide ions cannot be produced.

The oxidation conditions attained by the electrooxidation (ElectroFenton's reagent) process, of the organic components contained in the wastewater, permitted to obtain lower COD values, compared to those obtained using electrocoagu-

lation. In the other hand, at acidic conditions the Electro-Fenton method is much better in organic pollutant removal from wastewater^{20,36,37}. However, electrocoagulation process is capable for decolorization of C.I. reactive red 124 and decolorization pH of EC is convenient.

Effect of initial pH on electrode consumption

The electrode consumption values were calculated according to Faraday's law in following manner:

$$m_{\text{Fe}} = \frac{M \cdot I \cdot t}{z F} \cdot 3600 \quad (9)$$

where m_{Fe} is the amount of consumed iron (g), M is the molar mass (g mol⁻¹) (atomic mass of iron $A_r = 56$), z is the charge number ($z_{\text{Fe}} = 2$), I is current (A), F is Faraday's constant ($9.65 \cdot 10^4 \text{ s A mol}^{-1}$), t is the electrolysis time (h). Figure 6 shows the electrode consumption in kg per kg of dye removed in relation to initial pH in EC. As can be seen in Fig. 6, the lower electrode consumption values were obtained for $7 < \text{pH} < 10$ for 3 min electrolysis time at 2.030 mA cm⁻² current density and for $6 < \text{pH} < 10$ for 5 min electrolysis time at 1.351 mA cm⁻² current density. The minimum electrode consumption was 0.35 kg electrode per kg dye at 1.351 mA cm⁻² and pH 8 for 5 min electrolysis times.

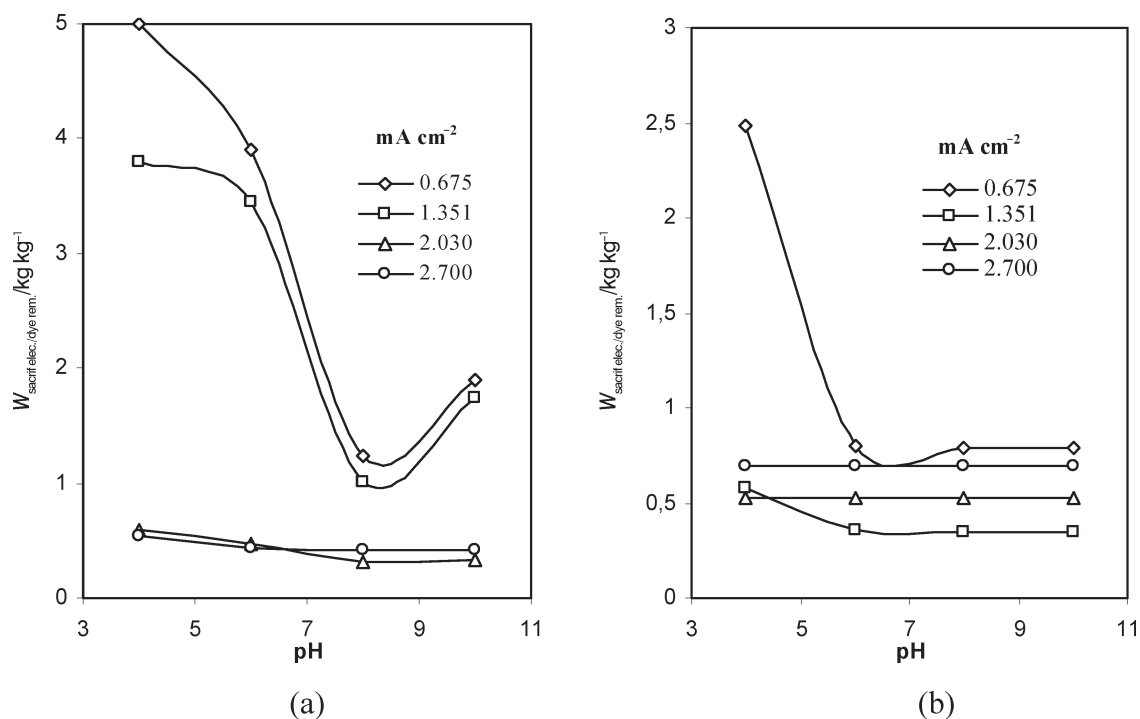


Fig. 6 – Effect of initial pH on electrode consumption. (a) Duration of electrolysis: $t = 3 \text{ min}$; (b) Duration of electrolysis: $t = 5 \text{ min}$ ($\gamma_o = 100 \text{ mg L}^{-1}$; $T = 298 \text{ K}$; $d = 2.5 \text{ cm}$; $\gamma_{\text{NaCl}} : 3 \text{ g L}^{-1}$; rotation speed: $n_r = 100 \text{ rpm}$)

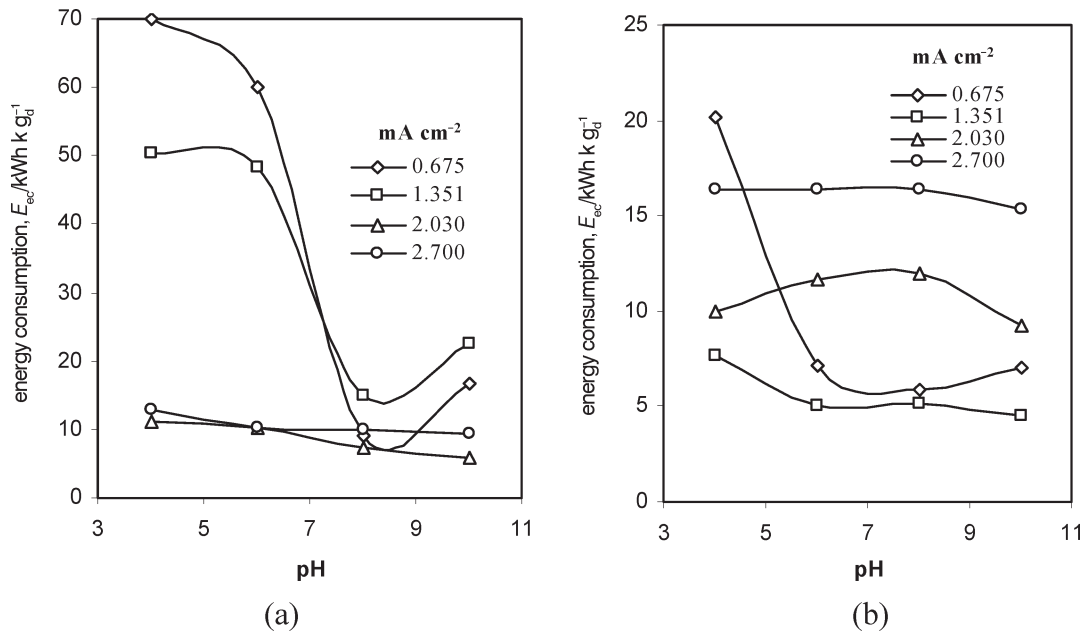


Fig. 7 – Effect of initial pH on energy consumption, per unit of dye removed (a) Duration of electrolysis: $t = 3$ min; (b) Duration of electrolysis: $t = 5$ min ($\gamma_o = 100$ mg L^{-1} ; $T = 298$ K; $d = 2.5$ cm; $\gamma_{NaCl} = 3$ g L^{-1} ; rotation speed: $n_r = 100$ rpm)

Effect of initial pH on energy consumption

Figure 7 shows the specific energy consumption versus pH for iron electrodes during the, EC expressed in kWh consumed per kg dye. As Fig. 7 shows, the minimum energy consumption was observed at $7 < \text{pH} < 10$ for 3 min at 2.030 mA cm^{-2} current density and at $6 < \text{pH} < 10$ for 5 min of electrolysis time at 1.351 mA cm^{-2} current density. The effect of pH on specific energy consumption per unit of removal efficiency is shown in Fig. 8. It can be seen that the minimum energy consumption appears for $6 < \text{pH} < 10$ at 5 min of electrolysis time and 1.351 mA cm^{-2} current density.

Effect of current density

Effect of current density on the removal efficiency of reactive dye

As shown in Fig. 9, the removal efficiency of the dye increased significantly with increasing of current density. With increasing current density the amount of oxidized iron is increased and consequently the amount of the hydroxyl polymers available for the attraction of the dye molecule are also increased. From Fig. 9, it is apparent that the removal efficiency was improved continuously with increasing current density and the maximum dye removal was observed at 2.030 mA cm^{-2} current density for pH 8 and 3 min of electrolysis time. As can be seen from Fig. 9 (b), for 5 min electrolysis time, the maximum dye removal was obtained at 1.351 mA cm^{-2} for pH 8. At pH 8, when the current density was increased from 1.351 mA cm^{-2} to 2.030

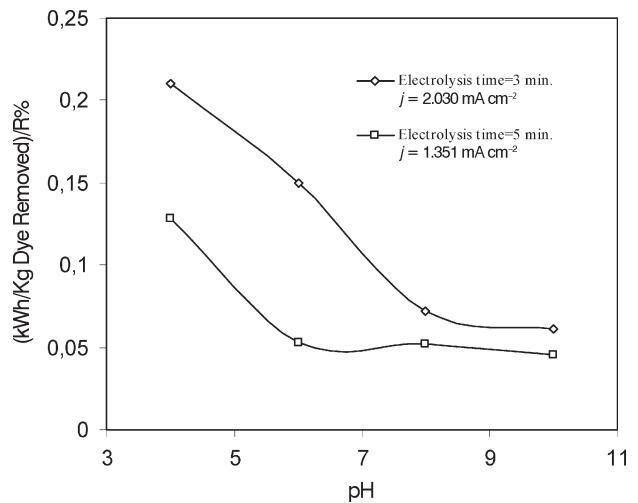


Fig. 8 – Effect of initial pH on energy consumption per unit of removal efficiency. ($\gamma_o = 100$ mg L^{-1} ; $T = 298$ K; $d = 2.5$ cm; $\gamma_{NaCl} = 3$ g L^{-1} ; rotation speed: $n_r = 100$ rpm)

mA cm^{-2} , the EC time was shortened from 5 to 3 min. As a result, it should be noted that the optimal dye removal was observed at 1.351 mA cm^{-2} , pH 8 and 5 min electrolysis time.

Effect of current density on electrode consumption

Figure 10 illustrates the effect of current density on electrode consumption expressed in kg per kg of dye removed. As shown in Fig. 10, minimum electrode consumption values were obtained at 2.030 mA cm^{-2} for 3 min electrolysis time and at 1.351 mA cm^{-2} for 5 min electrolysis time. The op-

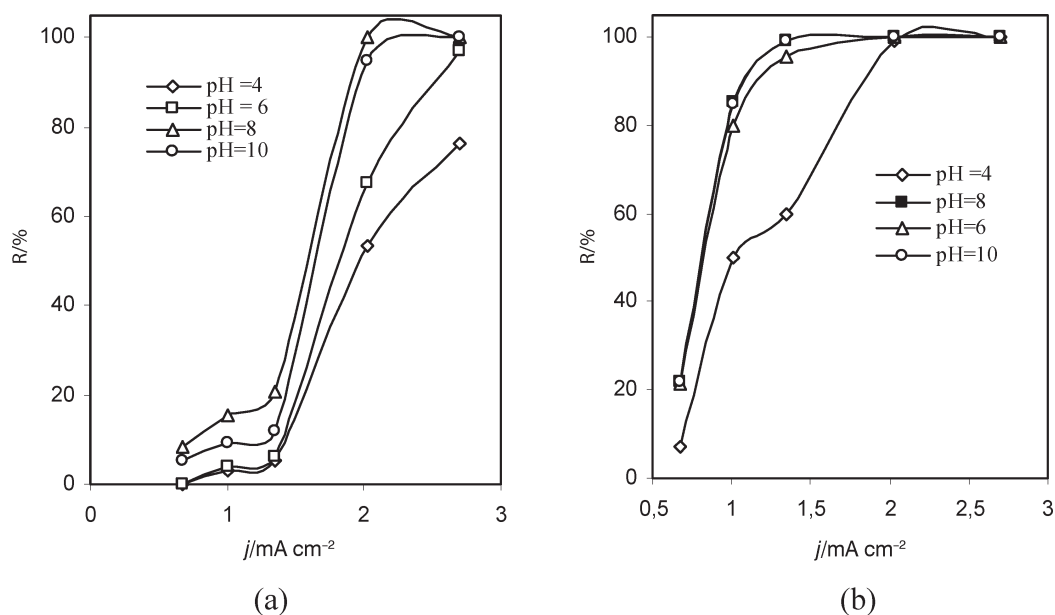


Fig. 9 – Effect of current density on the removal efficiency of reactive dye. (a) Duration of electrolysis: $t = 3$ min; (b) Duration of electrolysis: $t = 5$ min (γ_o : 100 mg L^{-1} ; $T = 298 \text{ K}$; $d = 2.5 \text{ cm}$; $\gamma_{\text{NaCl}} = 3 \text{ g L}^{-1}$; rotation speed $n_r = 100 \text{ rpm}$)

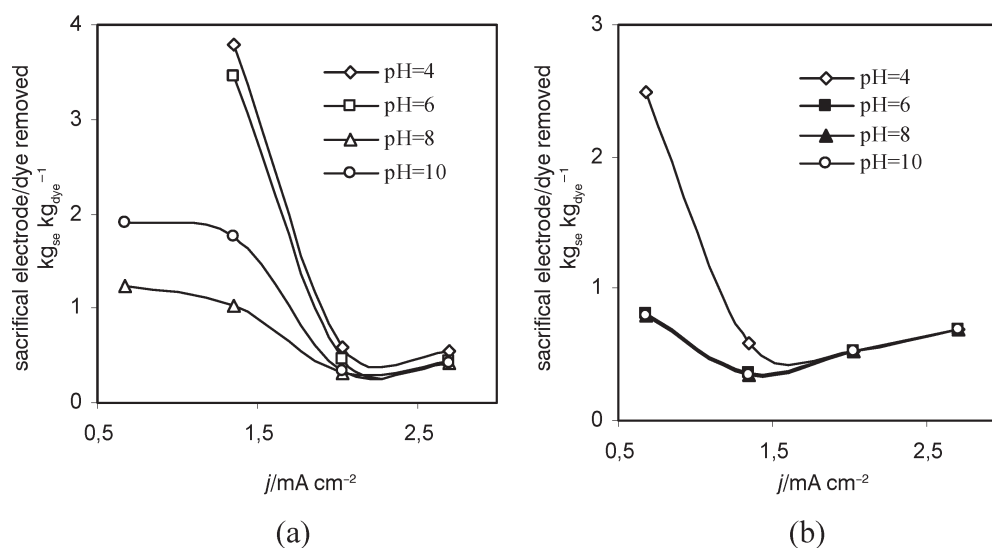


Fig. 10 – Effect of current density on electrode consumption. (a) Duration of electrolysis: $t = 3$ min; (b) Duration of electrolysis: $t = 5$ min (γ_o : 100 mg L^{-1} ; $T = 298 \text{ K}$; $d = 2.5 \text{ cm}$; $\gamma_{\text{NaCl}} = 3 \text{ g L}^{-1}$; rotation speed $n_r = 100 \text{ rpm}$)

imum current density corresponds to the end of the sharp decrease stage at pH 6 – 10 for 5 min electrolysis time and is equal to 1.351 mA cm^{-2} . Under these conditions, the electrode consumption is 0.35 kg per unit dye removed.

Effect of current density on energy consumption

The Effect of current density on energy consumption (kWh kg^{-1} dye removed) is shown in Fig. 11. Increase of the current density up to 2.030 mA cm^{-2} caused a decrease in power requirement for 3 min electrolysis time. In the same way, an increase

of current density up to 1.351 mA cm^{-2} caused a decrease in power requirement for 5 min electrolysis time. The minimum energy consumption was 7.52 kWh kg^{-1} dye at 2.030 mA cm^{-2} current density for 3 min electrolysis time and 4.54 kWh kg^{-1} dye at 1.351 mA cm^{-2} current density for 5 min electrolysis time in pH 8. The energy consumption in the high current density was increased by polarization. The effect of current density on energy consumption per unit of removal efficiency is shown in Fig. 12. Apparently, optimum current density for energy consumption is 1.351 mA cm^{-2} at 5 min electrolysis time and pH 8.

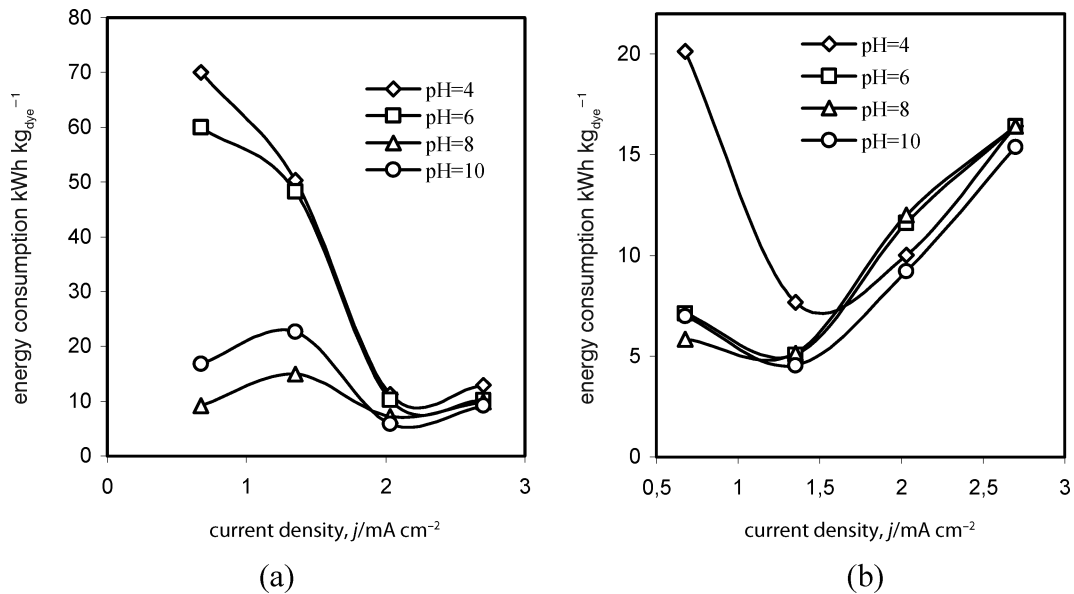


Fig. 11 – Effect of current density on energy consumption. (a) Duration of electrolysis: $t = 3$ min; (b) Duration of electrolysis: $t = 5$ min ($\gamma_o = 100$ mg L⁻¹; $T = 298$ K; $d = 2.5$ cm; $\gamma_{NaCl} = 3$ g L⁻¹; rotation speed $n_r = 100$ rpm)

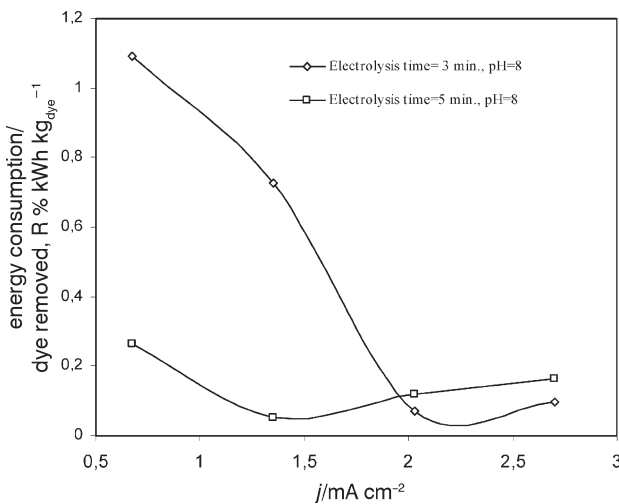


Fig. 12 – Effect of current density on energy consumption per unit of removal efficiency. ($\gamma_o = 100$ mg L⁻¹; $T = 298$ K; $d = 2.5$ cm; $\gamma_{NaCl} = 3$ g L⁻¹; rotation speed $n_r = 100$ rpm)

Effect of electrolysis time

As shown in Fig. 13, as the time of electrolysis increases comparable changes in the removed efficiency of C.I. reactive red 124 are observed. Figure 13 shows the relationship between the color removal and the electrolysis time. To explore the effect of operating time, the current density and pH were held constant. The color of the reactive dye was decreased as a function of elapsed time. After 5 min of electrolysis, the color removal efficiency reached a maximum at all pH values except for pH 4 and 0.675 mA cm⁻² current density; a 100 % color removal was achieved under this condition.

Effect of the initial concentration on the removal of reactive dye

As can be seen from Fig. 14, when the initial concentration of C.I. reactive dye 124 was increased from 100 to 500 mg L⁻¹, the retention time of the dye solution in the EC unit in order to achieve a 100 % removal efficiency was prolonged from 3 to 5.5 min. The reason for this is the lack of sludge for the adsorption of excess dye in high concentrations. It is necessary that the total amount of sludge is constant for all concentrations.

Effect of the amount of NaCl salt on the removal efficiency of reactive dye

In generally, NaCl is used to obtain the conductivity in EC process. The conductivity of the wastewater is adjusted to the desired levels by adding an appropriate amount of NaCl.^{30,38,39} The effect of NaCl concentration on the removal efficiency is shown in Fig. 15. When the concentration of NaCl salt in solution increases, conductivity of the solution and the current density increase. The higher ionic strength will generally cause an increase in current density at the same cell voltage or, equivalently, the cell voltage decreases with increasing wastewater conductivity at constant current density. Consequently, the necessary voltage to attain a certain current density will be diminished and the consumed electrical energy will decrease. It can be seen that there is an increase in the removal efficiency up to 100 % when the concentration of NaCl salt in the solution is 3.0 g L⁻¹. As shown in Fig. 15, the optimum salt concentration is 2.3 g L⁻¹. But,

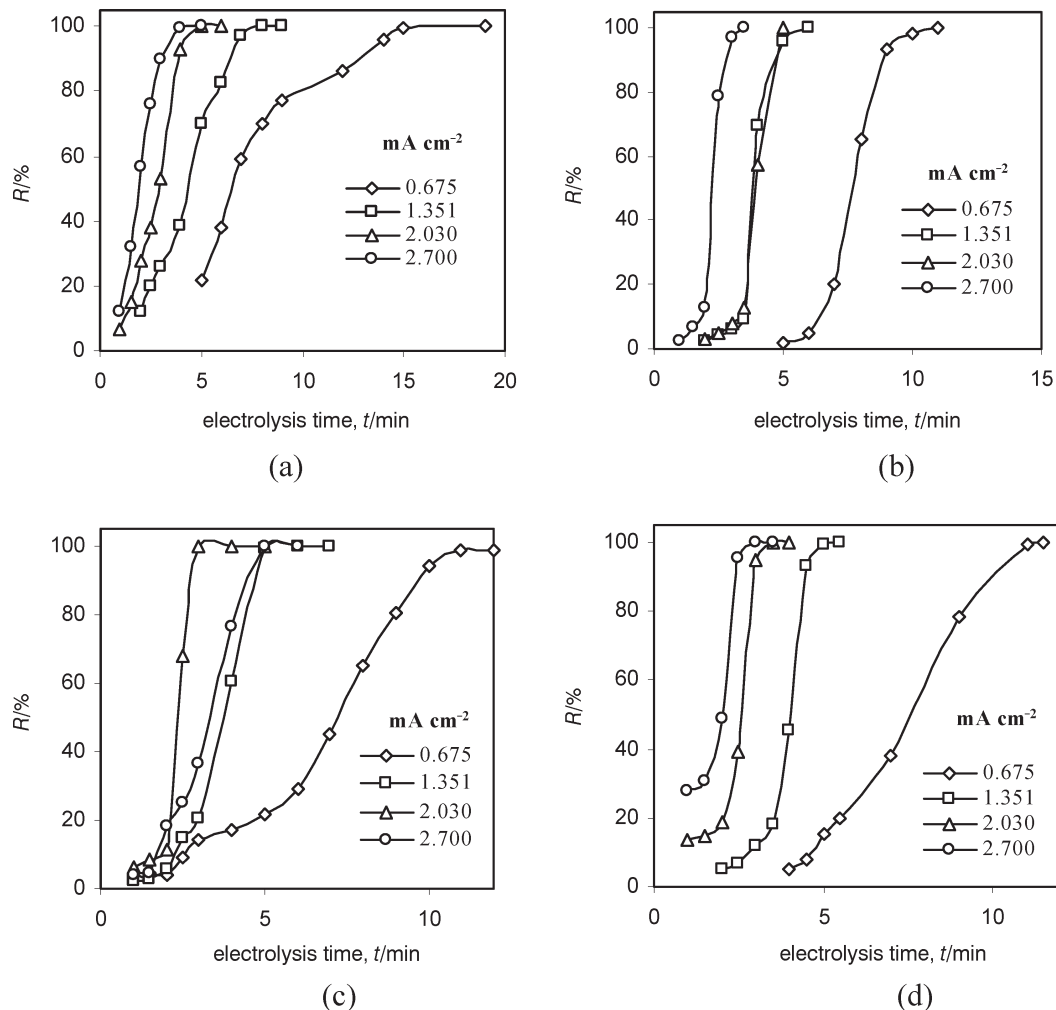


Fig. 13 – Effect of electrolysis time on the removal efficiency of the reactive dye. (a) pH 4; (b) pH 6; (c) pH 8; (d) pH 10 (γ_o : 100 mg L^{-1} ; $T = 298 \text{ K}$; $d = 2.5 \text{ cm}$; $\gamma_{\text{NaCl}} = 3 \text{ g L}^{-1}$; rotation speed: $n_r = 100 \text{ rpm}$)

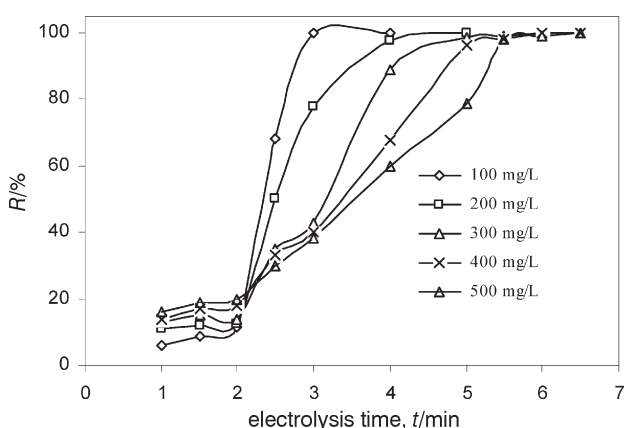


Fig. 14 – Effect of initial concentration on the removal efficiency of the reactive dye. (pH 8; $j = 1.351 \text{ mA cm}^{-2}$; $T = 298 \text{ K}$; $d = 2.5 \text{ cm}$; $\gamma_{\text{NaCl}} = 3 \text{ g L}^{-1}$; rotation speed: $n_r = 100 \text{ rpm}$)

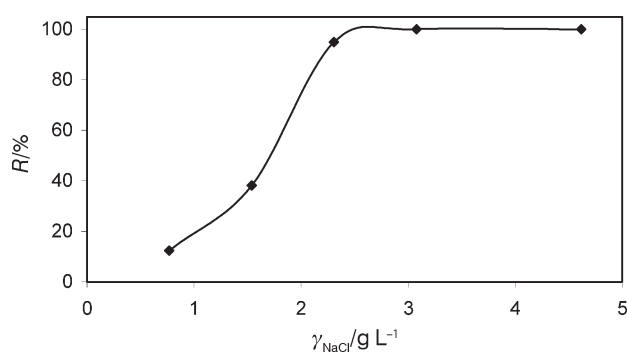


Fig. 15 – Effect of the amount of NaCl on the removal efficiency of reactive dye. (duration of electrolysis: $t = 3 \text{ min}$; pH 8; γ_o : 100 mg L^{-1} ; $T = 298 \text{ K}$; $j = 1.351 \text{ mA cm}^{-2}$; $d = 2.5 \text{ cm}$; rotation speed $n_r = 100 \text{ rpm}$)

Effect of the current density on the COD removal efficiency

this amount of salt was not enough for current density more than 1.351 mA cm^{-2} at the same cell voltage. In this respect, 3.0 g L^{-1} NaCl was used in the experiments.

Fig. 16 depicts the effect of current density on COD removal efficiency at 5 min. electrolysis time and pH 8. As shown in Fig. 16, the removal efficiency of COD increased significantly with increas-

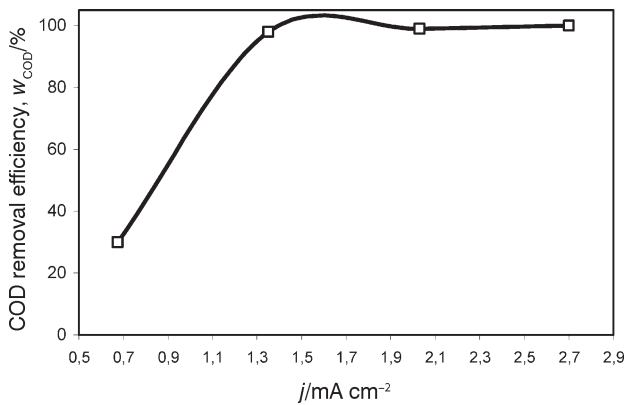


Fig. 16 – Effect of current density on the COD removal efficiency. (duration of electrolysis: $t = 5$ min; pH 8; $\gamma_o = 100$ mg L⁻¹; $T = 298$ K; $d = 2.5$ cm; $\gamma_{NaCl} = 3$ g L⁻¹; rotation speed: $n_r = 100$ rpm)

ing of current density like the variation of current density–dye removal efficiency. Its reason has been discussed in the section Effect of current density.

Modelling for calculation of the dye removal

The dye removal after 3 min of EC for the initial mass concentration of 100 mg L⁻¹ can be calculated according to

$$m_{\text{dye}} = m_{\text{Fe}} (k - n\gamma_{\text{res}}) \quad (10)$$

where m_{dye} is the mass (mg L⁻¹) removed from the dye solution for 3 min electrolysis time, m_{Fe} is the mass of dissolved iron during the electrolysis (g L⁻¹), γ_{res} is the residual mass concentration of dye (mg L⁻¹) for 3 min electrolysis time, the coefficient k denotes the dye removal capacity (mg dye per unit of g⁻¹ iron) and n is an other coefficient (L g⁻¹ iron). m_{Fe} was calculated from Faraday's law.

Eq. 10 corresponds simply to the mass balance of the dye (concentration removed = initial concentration – residual concentration). Also, the use of Faraday's law to calculate m_{Fe} is valid, provided that the current efficiency is 100 % (no parasitic reactions). The values of k and n were calculated from the slope and intercept of the linear plot, $m_{\text{dye}}/m_{\text{Fe}}$ vs γ_{res} and are represented in Table 2.

The values of k in Table 2 reveal that the k value at pH 8 is the greatest. This shows that the dye removal capacity (mg dye/g iron) gets its highest value at pH 8.

A relationship between equation (10) and Faraday's equation (9) can be derived:

$$m_{\text{dye}} = I \cdot 0.0803 (k - \gamma_{\text{res}}) \quad (11)$$

Eq. (11) shows that the dye removal (mg L⁻¹) increases linearly with current (I) and the k coeffi-

Table 2 – k and n constants for various pH values

pH	k	n	R^2
4	1695	16.29	0.96
6	1713	16.35	0.97
8	2067	17.32	1.00
10	2061	18.64	0.99

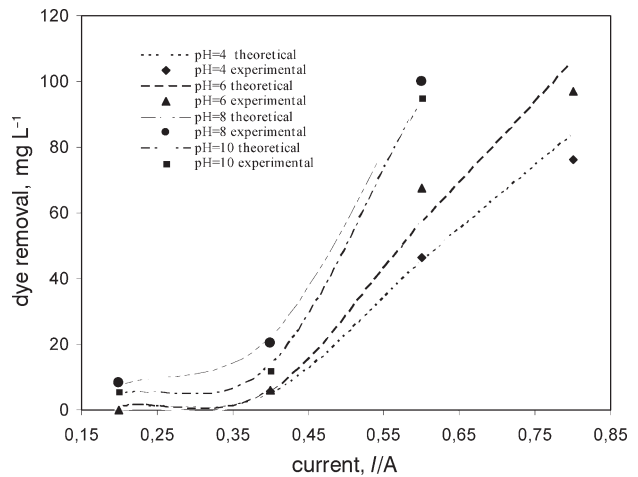


Fig. 17 – Effect of current on the removal amount of reactive dye. (duration of electrolysis: $t = 3$ min; $\gamma_o = 100$ mg L⁻¹; $T = 298$ K; $d = 2.5$ cm; $\gamma_{NaCl} = 3$ g L⁻¹; rotation speed: $n_r = 100$ rpm)

cient. The theoretical γ_{res} values for various pH values were calculated using equation (11). Figure 17 shows a comparison between the theoretical values and the experimental data. As can be seen in Fig. 17, the calculated values were found to generate a satisfactory fit to the experimental data.

Conclusions

The EC system successfully removes C.I. reactive dye 124. The mechanism concerning the removal of C.I. reactive dye 124 propose that the reactive group of dye actually may form a covalent bound with hydroxyl groups of ferric hydroxo complexes. The decolorization of the reactive dye using iron sacrificial anode was affected by the initial pH, the current density, the amount of NaCl and the initial dye concentration. The results showed that the dye was effectively removed at initial pH 8 when the initial concentration of dye was 100 mg L⁻¹. The results also indicated that the removal efficiency of the reactive dye was raised to 100 %. The optimal current density was 1.351 mA cm⁻² at pH 8 for an operating times of 5 min. The iron electrode

consumption was 0.35 kg electrode per kg dye at 1.351 mA cm⁻², pH 8 and 5 min electrolysis time. At these optimal conditions the power requirement and NaCl amount were 4.54 kWh kg⁻¹ dye and 2.3 g L⁻¹, respectively. Finally, a mathematical equation showing the relation between the amount of the dye removal and the current for 3 min electrolysis time and 100 mg L⁻¹ initial dye concentration at pH 8 was presented. The predictions of this mathematical model are in very good agreement to the experimental data.

References

1. Willcock, A., Brewster, M., Tincher, W., *American Dye Stuff Reporter* (1992) 15.
2. Do, J.-S., Chen, M.-L., *J. Appl. Electrochem.* **24** (1994) 785.
3. Sheng, H. L., Peng, L.C., *Water Res.* **28** (1994) 277.
4. Zoltek, J., Melear, E. L., *J. WPCF* **53** (1982) 679.
5. Morais, L. C., Freitas, O. M., Gonc Alves, E. P., Vasconcelos, L. T., Beça, C. G. G., *Water Res* **33** (1999) 979.
6. Özacar, M., Şengil, I. A., *Water Res.* **34** (2000) 1407.
7. Şengil, I. A., *Water Res.* **29** (1995) 1988.
8. Jiang, J. Q., Graham, J. D., *Environ. Technol.* **17** (1996) 937.
9. Özacar, M., Şengil, I. A., *J.Hazard. Mater.* **B98** (2003) 211.
10. Özacar, M., Şengil, I. A., *Adsorption* **8** (2002) 301.
11. Vik, E. A., Carlson, D. A., Eikum, A. S., Gjessing, E. T., *Water Res.* **18** (1984) 1355.
12. Alexandrova, L., Nedialkova, T., Nishkov, I., *Int. J. Mineral Processing.* **41** (1994) 285.
13. Chen, X., Chen, G., Yue, P. L., *Sep. Purif. Technol.* **19** (2000) 65.
14. Rhutdhawong, W., Chowwanapoonpohn, S., Buddhasukh, D., *Analytical Sciences* **16** (2000) 1083.
15. Pouet, M. F., Grasmick, A., *Water Sci. Tech.* **31**(1995) 275.
16. Tsai, C. T., Lin, S. T., Shue, Y. C., Su, P. L., *Water Res.* **31** (1997) 3073.
17. Lin, S. H., Shyu, C. T., Sun, M. C., *Water Res.* **32** (1998) 1059.
18. Balaubramanian, N., Madhavan, K., *Chem. Technol.* **24** (2001) 5.
19. Barrera-Diaz, C., Palomar-Pardave, M., Romero-Romo, M., Martinez, S., *J. Appl. Electrochem.* **33** (2003) 61–71.
20. Barrera-Diaz, C., Urena-Nunez, F., Campos, E., Palomar-Pardave, M., Romero-Romo, M., *Rad. Phys and Chem* **67** (2003) 657–663
21. Picard, T., Cathalifaud-Feuillade, G., Mazet, M., Vandensteendam, C., *J. Environ. Monit.* **2** (2000) 77.
22. Mollah, M. Y. A., Schennach, R., Parga, J. R., Cocke, D. L., *J. Hazard. Mater.* **B84** (2001) 29.
23. Rajeshwar, K., Ibanez, J. G., Swaine, G. M., *J. Appl. Electrochem.* **24** (1994) 1077.
24. Riveiro, A. B., Mateus, E. P., Ottosen, L. M., Bech-Nielsen, G., *Environ. Sci. Technol.* **34** (2000) 781.
25. Lin, S. H., Peng, C. F., *Water Res.* **30** (1996) 587.
26. Lin, S. H., Peng, C. F., *Water Res.* **28** (1994) 277.
27. Ciardelli, G., Ranieri, N., *Water Res.* **35** (2001) 567.
28. Lin, S. H., Peng, C. F., *Water Res.* **28** (1994) 277.
29. Xiong, Y., Strunk, P. J., Xia, H., Zhu, X., Karlsson, H. T., *Water Res.* **35** (2001) 4226.
30. Daneshvar, N., Ashassi-Sorkhabi, H., Tizpar, A., *Sep. Purif. Technol.* **31** (2003) 153.
31. Gurses, A., Yalçın, M., Dogar, C., *Waste Manag.* **22** (2002) 491.
32. Johnson, P. N., Amithararajah, A., *J.AWWA* **5** (1983) 232.
33. Başer, I., Inanici, Y., *Dyestuff Chemistry*, Marmara University, Turkey, 1990, pp 147–149.
34. Martínez, S. A., Rodríguez M. G., Barrera C., *Water Science & Technology*, **42** (2000) 55.
35. Beck, R. T., *J. Appl. Electrochem.* **129** (1982) 2412.
36. Brillas, E., Casado, J., *Chemosphere*, **47** (2002) 241.
37. Brillas, E., Boye, B., Banos, M. A., Calpe, J. C., Garrido, J. A., *Chemosphere*, **51** (2003) 227–235.
38. Kobya, M., Ot, C., Bayramoglu, M., *J. Appl. Electrochem.*, **100** (2003) 163–178.
39. Ot, C., Bayramoglu, M., Kobya, M., *Ind.Eng. Chem. Res.*, **42** (2003) 3391–3396.
40. Bektas, N., Akbulut, H., Inan, H., Dimoglo, A., *J. Hazard. Mater.* **106B** (2004) 101–105.
41. Lewis, D. M., Wang, J. C., *Dyes and Pigments*, **39** (1998) 111.
42. Music, S., Genilson, P., Santana, G. P., Goran, S., Garg, V. K., *Croatia Chemica Acta* **72** (1999) 87.
43. Ishikawa, T., Kondo, Yasukawa, Y. A., Kandori, K., *Corrosion Sci.* **40** (1998) 1239.
44. Zielińska, B., Grzechulska, J., Morawski, A. W., *J. Photochem. Photobiol. A: Chemistry* **157** (2003) 65.

